Geoderma 429 (2023) 116243

Contents lists available at ScienceDirect

Geoderma

journal homepage: www.elsevier.com/locate/geoderma

Similar strong impact of N fertilizer form and soil erosion state on N_2O emissions from croplands

Shrijana Vaidya [a,*], Mathias Hoffmann [a], Maire Holz [a], Reena Macagga [a], Oscar Monzon [a], Mogens Thalmann [a], Nicole Jurisch [a], Natalia Pehle [a], Gernot Verch [b], Michael Sommer [c,d], Jürgen Augustin [a]

[a] Leibniz Center for Agricultural Landscape Research (ZALF), Working Group for Isotope Biogeochemistry and Gas Fluxes, Eberswalder Str. 84, 15374 Müncheberg, Germany
[b] Leibniz Center for Agricultural Landscape Research (ZALF), Experimental Infrastructure Platform, Steinfurther Straße 14, 17291 Prenzlau, Germany
[c] Leibniz Center for Agricultural Landscape Research (ZALF), Working Group for Landscape Pedology, Eberswalder Str. 84, 15374 Müncheberg, Germany
[d] University of Potsdam, Institute of Environmental Science and Geography, Karl-Liebknecht-Str.24-25, 14476 Potsdam, Germany

ARTICLE INFO

Handling Editor: Daniel Said-Pullicino

Keywords:
Manual chamber
Soil erosion
N fertilization form
Nitrous oxide emission
Soil

ABSTRACT

Soil erosion affects 20% of croplands worldwide. However, understanding the effect of soil erosion on N_2O emissions, which is one of the most potent greenhouse gases, is still limited. This limitation is likely because the small-scale differences in soil properties and fertility induced by erosion (i.e. ranges of erosion states) have barely been considered in studies quantifying N_2O emissions from croplands. There are, however, indications that the erosion state itself strongly impacts N_2O emission, similar to the N fertilizer form. Therefore, our investigations aimed to further explore these indications.

We measured N_2O fluxes for three years and at five sites within an erosion affected field experiment. N_2O emissions were quantified using a manual chamber system. Three sites were established on a summit position (Albic Luvisol; non-eroded) but differed in N fertilizer forms (organic biogas fermented residues, calcium ammonium nitrate and a mixture of both fertilizers). Two additional sites were established on an extremely eroded soil (Calcaric Regosol) and wet depositional soil in a depression (Endogleyic Colluvic Regosol) to measure the effect of soil erosion states on N_2O emissions. Both additional sites were fertilized with calcium ammonium nitrate only.

In case of the non-eroded soil (summit), organic fertilization resulted in the highest cumulative N_2O emission (6.2 ± 0.21 kg N_2O-N/ha y^{-1}) compared to mixed (5.5 ± 0.18 kg N_2O-N/ha y^{-1}) and mineral (1.9 ± 0.17 kg N_2O-N/ha y^{-1}) fertilization. These high emissions were probably caused by soluble C and N substrates from organic fertilizer, resulting in microbial activities favoring high N_2O emissions. Regarding the erosion status, we observed the highest N_2O emissions in the depositional soil (2.8 ± 0.21 kg N_2O-N/ha y^{-1}), followed by the non-eroded (1.9 ± 0.17 kg N_2O-N/ha y^{-1}) and the extremely eroded soil (0.6 ± 0.03 kg N_2O-N/ha y^{-1}). These differences in N_2O emissions were mainly due to the site-specific, erosion induced differences in soil properties such as soil texture, soil organic C and total N contents and stocks, water-filled pore space and soil pH. These results indicate that soil erosion state may indeed be of similar importance, as N fertilizer form, for the magnitude of N_2O emissions from croplands.

1. Introduction

Globally, around 20 % of cropland is affected by soil erosion (Prăvălie et al., 2021), resulting in reduced soil fertility, crop productivity and food security. This is caused not only by the general, lateral transfer of soil organic matter and nutrients from the arable land to the water bodies but also by the formation of small-scale patterns within cropland areas that differ greatly from one another due to erosion-induced soil removal or deposition. Low soil fertility in eroded croplands can be exacerbated by tillage operations if subsoil with low carbon (C) and nutrient content is mixed into the remaining topsoil (Berhe et al., 2018; Doetterl et al., 2016; Nie et al., 2019; Van Oost et al., 2007).

* Corresponding author.
E-mail address: shrijana.vaidya@zalf.de (S. Vaidya).

https://doi.org/10.1016/j.geoderma.2022.116243
Received 26 March 2022; Received in revised form 25 October 2022; Accepted 28 October 2022
Available online 5 November 2022

Information on erosion impact on the importance of cropland as a source and sink of climate-relevant trace gases is still very incomplete. So far, the focus has been mainly on the influence the soil erosion status might have on carbon dioxide (CO_2) fluxes (Doetterl et al., 2016; Hoffmann et al., 2017; Lal, 2019; Vaidya et al., 2021). For instance, Hoffmann et al. (2018) reported that the C dynamics are driven by soil erosion states and plant phenology rather than N fertilizer form. However, in the case of nitrous oxide (N_2O), which is one of the most potent greenhouse gases, with a global warming potential 273 times greater than CO_2 (IPCC, 2022), there is very little information on this.

Agriculture is the principal anthropogenic contributor of increasing atmospheric N_2O concentration, responsible for approximately 60 % of total N_2O emission (Ciais et al., 2013; Mbow et al., 2019; Tian et al., 2020). The rising global demand for food, fodder and fuel triggers higher N_2O emission due to agricultural intensification with increasing use of mineral and organic nitrogen (N) fertilizers (Lassaletta et al., 2016; Pradhan et al., 2015; Reay et al., 2012). The level of N_2O emission rate is strongly determined by the amount of N fertilization. With increasing N fertilization, the amount of ammonium (NH_4^+) and nitrate (NO_3^-) in the soil increases, the most important substrates of the microbial processes responsible for N_2O formation, such as nitrification and denitrification. (Bouwman et al., 2002; Pareja-Sánchez et al., 2020; Shcherbak et al., 2014). The N_2O emission rate, however, varies according to N fertilizer forms and amount (Gelfand et al., 2016; Kudeyarov, 2020; Millar et al., 2010). The addition of labile C in organic fertilization can increase denitrification in two ways: first, the microbial respiration rate increases, consuming soil oxygen and creating the anaerobic conditions required for denitrification; second, it also increases the supply of readily degradable C, which, along with NO_3^-, is also needed as a substrate for denitrification. Due to this reason, organic fertilizers (e.g., liquid dairy cattle or poultry manure) which contain large amounts of labile C and N, might increase N_2O emission compared to mineral fertilizers (Huang et al., 2020; Van Groenigen et al., 2004).

There are some indications that the erosion state may exert an influence similar to that of N fertilization on N_2O fluxes. On the one hand, erosion can lead to extremely high differences in soil organic C (SOC) and total N (N_t) content and stocks in the soil at small scales (Kumar et al., 2019; Navas et al., 2012; Wang et al., 2020; Xue et al., 2013; values differ by a factor of 2 to 10). While topsoil erosion sites are characterized by very low SOC and N_t content and stocks (e.g. total C concentration <0.5 %; total N concentration <0.04 %), topsoil deposition sites often have much higher SOC and N_t content and stocks (e.g. total C concentration >1.5 %; total N concentration >0.5 %). On the other hand, erosion state, mostly coupled with a specific terrain position, indicates substantial differences in the water regime of the soils. Overland flow into concave landscape positions does not bring just sediments but water. This leads to wetter conditions compared to drier, eroded soils at convex landscape positions. Furthermore, a capillary rise of groundwater in depositional soils leads to higher soil moisture in topsoil, which influences soil C and N transformation processes and N_2O formation (Kong et al., 2022; Mbonimpa et al., 2015; Nie et al., 2019; Weintraub et al., 2015).

In fact, the few existing investigations about N_2O emissions on eroded cropland indicate an impact of terrain position on N_2O emissions (Ashiq et al., 2021; Negassa et al., 2015; Vilain et al., 2010). In some of these studies, higher N_2O emissions were observed in the depression than in the shoulder position (Corre et al., 1996; Gu et al., 2011; Vilain et al., 2010; Ashiq et al., 2021). However, the evaluation was either done only on two terrain positions (depression and shoulder), or the terrain positions were situated in separate fields with different land use, which hampers the interpretation of these results. For example, Ashiq et al. (2021) investigated the impact of various terrain positions on N_2O emissions on a landscape scale and did not observe a clear effect of terrain position on N_2O fluxes. In addition to that, information regarding the influence of N fertilizer form coupled with soil erosion state is often limited to changes in crop growth and yield (Lin et al., 2019) or C dynamics (Hoffmann et al., 2018; Li et al., 2019). To date, it has not been investigated whether erosion status actually has a similar strong effect on N_2O emissions as the form and rate of N fertilization. However, such information is urgently needed to correctly assess the role of eroded cropland as a source of N_2O and develop effective management options to reduce N_2O emissions and thus, the climate impact of land use.

We conducted N_2O measurements on an eroded cropland over three years from May 2010 to May 2013 in order to compare the impact of N fertilizer forms and erosion states on N_2O emissions. The tested hypotheses were: (1) At the non-eroded soil, N_2O fluxes are higher from organic (ORG) and organic + mineral (MIX) fertilized soil compared to mineral (MIN) fertilized soil. (2) The three distinct erosion states (depositional, non-eroded, extremely eroded soil) have a similar influence on N_2O fluxes as N fertilizer forms (ORG, MIX and MIN).

2. Materials and methods

2.1. Study area and experimental setup

The study area is located within the erosion affected study area "CarboZALF-D" (6 ha), situated in the hummocky arable ground moraine landscape of northeast Germany (53° 23′ N, 13° 47′ E; ~50–60 m a.s.l) (Fig. 1).

The long-term average annual air temperature and precipitation are 9.1 °C and 505 mm, respectively (2005 to 2020; ZALF research station, Dedelow). The soils were formed from sandy to marly glacial and glaciofluvial deposits through soil erosion, with distinct soil profiles representing soil erosion states (Sommer et al., 2016, 2008). Terrain positions present at the "CarboZALF-D" experimental field vary from relatively flat summits and depressions with a gradient of approximately 2 %, across longer slopes with a medium gradient of approximately 6 %, to short and rather steep slopes with a gradient of up to 13 % (Hoffmann et al., 2017).

We established a fractional, two-factorial experiment to investigate the influence of erosion state and N fertilizer form on N_2O emissions (Fig. 1). Three study sites were located on a summit [Albic Luvisols (LVa non-eroded soil)]. Here, the form of applied N fertilizer differed [83 % organic (ORG) biogas fermented residues (BFR), 100 % mineral (MIN) calcium ammonium nitrate (CAN), and a mixture (MIX) of both fertilizers (57 % MIN + 43 % ORG)]. The real proportion of organic fertilizer in the ORG fertilized site was 83 % due to an unusual strong winter in 2012 which required an additional mineral fertilization at all sites to minimize crop yield loss through cold-affected crops (For details, see Table A2). Two additional sites were established on an extremely eroded steep slope with Calcaric Regosols (RGca) and in a depression with Endogleyic Colluvic Regosols (RGco) [soil classification according to IUSS Working Group (WRB, 2015)]. Both were treated with 100 % CAN. The RGco in drainless lower terrain positions contained the largest organic matter and nutrient stocks with a groundwater level (GWL) approximately 80 cm below the surface. The crop rotation of Maize (*Zea mays* L.) – Maize (*Zea mays* L.) – Winter rye (*Secale cereale* L.) – Sorghum (*Sorghum bicolor*) – Triticale (*Triticosecale*) was identical for all sites. After each harvest, all sites were ploughed (25 cm), followed by fertilizer incorporation and seedbed preparation using a rotary cultivator.

2.2. Fertilization

ORG originated from maize silage and co-fermented with cattle slurry was applied using a manure trailer (10 m^3) with a drag hose. Right after application, ORG was directly incorporated into the soil using a rotary cultivator. The amount of ORG applied to LVa-ORG and LVa-MIX was determined to match the amount of mineral N fertilizer application at LVa-MIN, RGca-MIN and RGco-MIN. Therefore, it was assumed that the plant-available N (PAN) accounted for 70 % of the N_t in ORG (Buchen-Tschiskale et al., 2020; Forrestal et al., 2016). MIN was applied using a pneumatic fertilizer spreader and incorporated into the soil to a

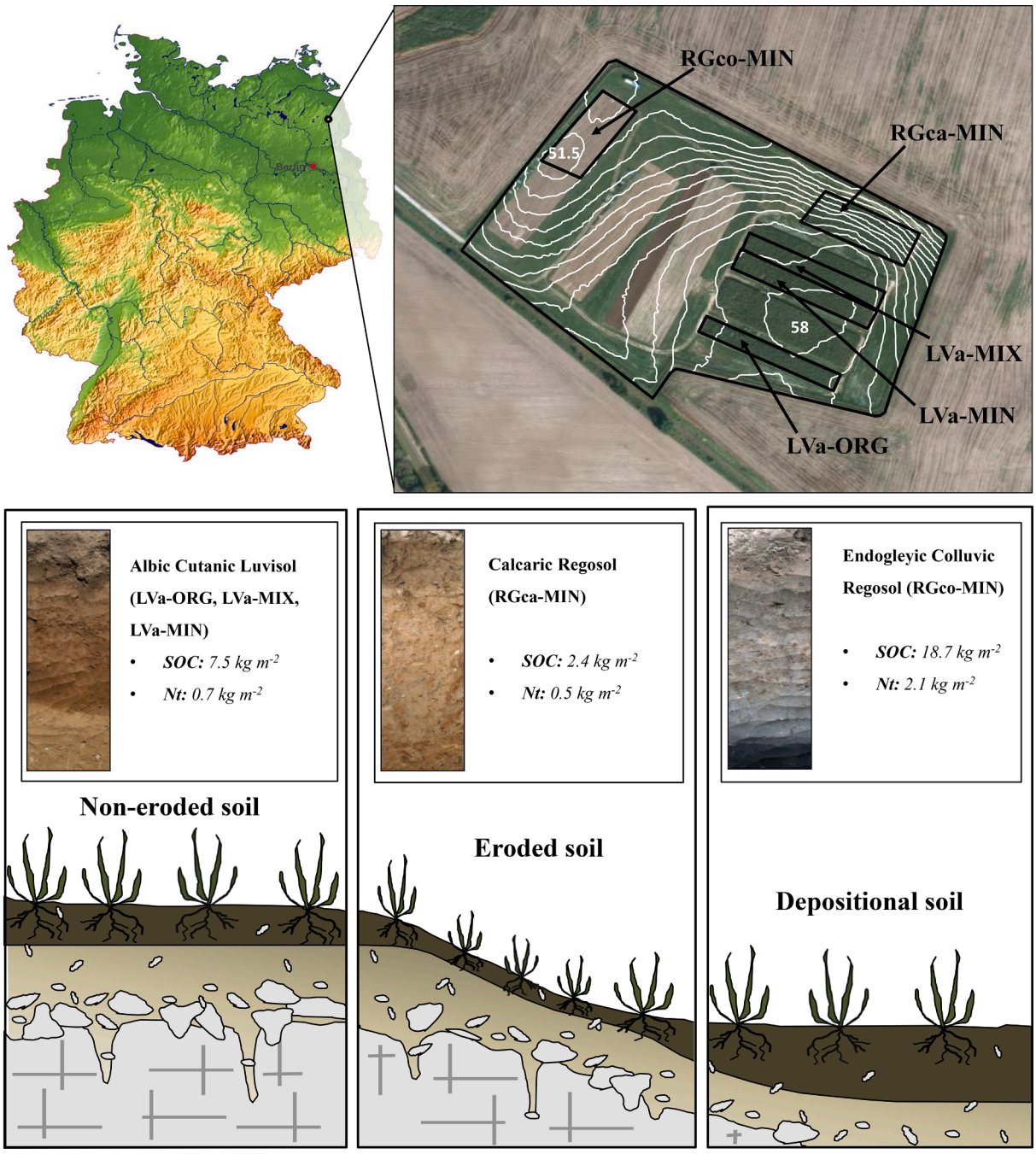

Fig. 1. (Top) Location of the study area CaboZALF-D near Dedelow, Uckermark region, NE Germany (53°23 N, 13°47E), showing the position of the five measurement sites representing the three different soil erosion states and N fertilizer treatments; (bottom) idealized schematic representation of erosion states characterized by distinct soil profiles; Albic Cutanic Luvisol (LVa; non-eroded soil), Calcaric Regosol (RGca; extremely eroded soil), Endogleyic Colluvic Regosol (RGco; depositional soil). The ORG, MIN and MIX represent organic, mineral and mixture of organic and mineral fertilizer forms, respectively (see Section 2.1 for further details). SOC and N_t stocks represent total sums of soil horizon-wise analyzed stocks.

depth of 20 cm within a week after application using a cultivator. Due to a strong winter in 2012 (temperatures below −20 °C), additional MIN was applied at all five sites to minimize crop yield loss through cold-affected crops. Further details about crop management and applied fertilizers for P, K, Mg, and S can be found in Table A2.

2.3. N_2O flux measurements

Nitrous oxide fluxes were measured using a non-flow-through non-steady-state (NFT-NSS) manual closed chamber system (Livingston and Hutchinson, 1995). The chambers [thickness: 2 mm; volume: 0.296 m^3; area: 0.5625 m^2 (0.75 m × 0.75 m)] used in the study were made out of white PVC and equipped with four vents at the top to connect pre-evacuated glass bottles (volume: 60 ml) for air sampling. Additional white PVC extensions (volume: 0.296 m^3) were used to adjust chamber volume for plant height. We performed N_2O flux measurements for three repetitive plots per site (pseudo-replication) by deploying the chambers on a PVC frame inserted 5 cm deep into the soil. Frames were removed prior and placed again directly after farming practices such as soil preparation, fertilization and harvest. Chambers and extensions were sealed at the bottom using rubber gaskets to assure airtight closure and prevent leakage (Hoffmann et al., 2018). In addition, chambers were

fixed to the frame using elastic belts. Chamber deployment time was 60 min, with gas samples taken in a 20 min interval, resulting in four gas samples per flux measurement. Hence, we collected 12 samples from each site during one measurement campaign. Gas samples were subsequently analyzed for CO_2 and N_2O concentrations using a gas chromatography system (GC-14A and GC-14B, Shimadzu Scientific Instruments, Japan) equipped with an electron capture detector (Loftfield et al., 1997). In general, N_2O flux measurements were carried out every 2 to 4 weeks throughout the study period. Additional measurements were conducted to more accurately cover events with expected peaks in N_2O fluxes (e.g., Barton et al., 2015). This included daily N_2O flux measurements up to one week following fertilization, with a decreasing frequency afterwards. In addition, sampling frequency increased after heavy rain and frost-thaw events.

2.4. N_2O flux calculation, estimation of annual emission and emission factor

Prior to N_2O flux calculation, N_2O concentration development over chamber closure was checked for reliability using the expected CO_2 concentration increase (opaque chamber; ecosystem respiration) during the same measurement as a quality criterion (Jurasinski et al., 2014). In the case of decreasing CO_2 concentrations over measurement time, measurements were considered biased and excluded from further analysis. To increase the robustness of flux calculation, we aggregated the determined concentrations of all three parallel chamber measurements per site and measurement day to one flux data set (n = 12) (Huth et al., 2018).

Nitrous oxide fluxes (F; μmol m^{-2} s^{-1}) were calculated according to the ideal gas law (Eq. (1)) and based on the often used assumption of a linear concentration increase during chamber enclosure (e.g., Barton et al., 2008; Huth et al., 2018; Jamali et al., 2016; Ussiri and Lal, 2012).

While the use of linear regression can often lead to the underestimation of fluxes, the linear regression based flux estimates are less sensitive to random errors (Venterea et al., 2020).

$$F = \frac{pV}{RTA} \cdot \frac{dc}{dt} \quad (1)$$

where p denotes the ambient air pressure (Pa), V denotes the chamber volume (m^3), R denotes the gas constant (8.314 m^3 Pa/K mol^{-1}), T denotes temperature inside the chamber (K), A denotes the chamber basal area (0.5625 m^2) and dc/dt denotes the slope of the linear N_2O concentration change in chamber headspace over measurement time (s^{-1}). Outliers in the aggregated data set for one flux measurement were identified, using six times the interquartile range (IQR) of regression residues as outlier criteria.

Nitrous oxide emission estimates were derived through simple linear interpolation of measured N_2O fluxes, thus assuming a linear change between fluxes of two consecutive measurement campaigns. We estimated the uncertainty of the measured N_2O emissions by using the error prediction algorithm described in detail by Huth et al. (2018).

Annual emission factors (EF, %) for N_2O were calculated following Dobbie and Smith (2003) and Jungkunst et al. (2006) as the percentage of total annual N_2O emission (kg N_2O-N ha^{-1}) to applied N fertilizer (kg N ha^{-1}). In accordance with both studies, no correction for background emission was performed.

2.5. Auxiliary measurements and soil analysis

In addition to N_2O flux measurements, we recorded environmental variables such as air pressure, air temperature, wind speed, wind direction and precipitation (WXT520 weather transmitter, Vaisala, Helsinki, Finland). We measured volumetric soil water content (SWC) with Frequency Domain Reflectometer (FDR) at reference soil profiles (15 cm depth). The measured % SWC was converted to water-filled pore space (% WFPS) for the three distinct erosion states using the bulk and particle density of the specific soil erosion state (AP horizon).

$$\%\text{WFPS} = \frac{\text{Soil Water Content}}{\text{Porosity}} \quad (2)$$

(Porosity = 1-bulk density/particle density); particle density = 2.65 mg m^{-3} (theoretical assumption (Gu et al., 2013; Lind et al., 2019; Vilain et al., 2010)).

Prior to the study, soil physical and chemical analyses for all three erosion states (LVa, RGca and RGco) were performed (Table 1). Undisturbed soil cores (100 cm^3) were taken in the middle of soil horizons and dried at 105 °C for determination of bulk density (BD). Bulk soil material was taken for each soil horizon, air dried, gently crushed and sieved (2 mm) to obtain the fine fraction (particle size <2 mm) as well as the coarse fraction (>2 mm, gravel). The particle size distribution of the fine fraction was determined by a combined wet sieving (>63 μm) and pipette (<20 μm) method (Schlichting et al., 1995). Pre-treatment for particle size analysis was done by (i) wet oxidation of organic matter using hydrogen peroxide (H_2O_2) (10 vol%) at 80 °C, (ii) carbonate dissolution with 0.5 N hydrochloric acid (HCl) (80 °C) and (iii) dispersion by shaking the sample end over end for 16 h with a 0.01 M tetrasodium pyrophosphate ($Na_4P_2O_7$)-solution (Schlichting et al., 1995). The total C and N_t content were determined by elementary analysis (TruSpec CNS analyzer, LECO ltd., Mönchengladbach, Germany) using carbon dioxide via infrared detection after dry combustion at 1250 °C (DIN ISO 10694, 1996). $CaCO_3$ was determined conductometrically using the Scheibler apparatus (Schlichting et al., 1995). Soil pH was determined on soil material <2 mm in a 0.01 M $CaCl_2$ solution with a TitraMaster 85 (Radiometer Analytical SAS, Lyon, France). During the growing season, soil samples were taken at different depths (0–30 cm, 30–60 cm, 60–90 cm) and extracted with 0.0125 M $CaCl_2$ solution (ratio 1:4) and analyzed for NH_4^+-N and NO_3^--N concentrations using spectrophotometry (VDLUFA, 1991) with a continuous flow analyzer (Skalar Analytics, CFA-SAN, Breda, Netherlands).

2.6. Statistical analysis

We checked for homogeneity of variances in derived N_2O fluxes (pseudo-replicates) among the three N fertilizer forms within the same soil erosion states (LVa-ORG, LVa-MIX, LVa-MIN) and the three distinct soil erosion states with mineral fertilizer application (LVa-MIN, RGca-MIN, RGco-MIN), using Bartlett's test. To achieve the normality and homogeneity of variances required for the one-way ANOVA, we transformed the measured N_2O fluxes logarithmically. We tested the differences in N_2O fluxes between the N fertilizer forms and soil erosion states with a one-way ANOVA followed by post-hoc multiple comparisons using Tukey's HSD method (significance level $p < 0.05$). In addition, soil temperature and %WFPS measured at the three distinct erosion states during the study period were tested for differences using the non-parametric two-sample Wilcoxon rank-sum test (significance level $p < 0.05$). Due to pseudo-replicates resulting from difficulties to replicate hillslope erosion and depositional sites, caution was applied in the inference of the statistical results.

3. Results

3.1. Environmental conditions

The average annual weather conditions during the study (2010 to 2013) were similarly warm (9.2 °C) but more humid (549 mm) compared to the long-term average annual air temperature of 9.1 °C and precipitation of 505 mm (2005 to 2020, ZALF research station, Dedelow). The mean daily air temperature showed a clear seasonal pattern. The range was between −17.5 °C in February 2012 and 27 °C in July 2010 (Fig. 2a).

Table 1
Soil types and erosion states induced by terrain position at the experimental sites as well as their physical and chemical properties. The properties related to the % soil texture are given for coarse, medium and fine sand (cs, ms, fs), coarse, medium and fine silt (csi, msi,fsi) and clay.

Soil types (WRB)	Horizon	Depth cm	>2 mm wt.-%	Bulk density Mg m^{-3}	Fine-earth mass kg m^{-2} 1 m^{-1}	cs	ms	fs	Csi	msi	fsi	clay	pH ($CaCl_2$)	SOC stocks kg m^{-2}	N_t stocks kg m^{-2}	C/N
						wt.-% of humus-/carbonate-free fine-earth (<2 mm)										
Albic Luvisol (Cutanic), non-eroded	Ap	0–31	3	1.76	533	4	22	33	18	9	5	9	5.53	4.13	0.41	10
	E	31–45	2	1.79	245	5	19	27	18	13	8	10	6.19	0.74	0.07	11
	Bt/E	45–62	4	1.67	272	4	18	26	16	11	8	16	6.37	0.81	0.06	13
	Btg1	62–90	2	1.76	484	4	19	28	14	9	8	19	6.79	1.40	0.13	11
	Btg2	90–135	2	1.73	169	3	20	31	14	10	6	16	7.24	0.45	0.04	11
Calcaric Regosol (Densic), extremely eroded	Ap	0–15	4	1.54	222	2	18	43	14	7	5	10	7.62	0.94	0.13	7
	CBkl1	15–28	4	1.68	209	5	20	38	13	8	4	11	7.63	0.73	0.13	6
	CBkl2	28–83	5	1.81	947	4	23	35	11	9	5	13	7.71	0.57	0.15	4
	CBkl3	83–200	4	1.83	299	4	23	35	12	8	6	12	7.74	0.18	0.05	4
Endogleyic Colluvic Regosol (Arenic), depositional	Ap	0–30	1	1.58	469	4	23	32	18	8	5	10	6.31	6.86	0.76	9
	Ab	30–58	1	1.66	461	3	17	31	19	11	6	13	6.85	4.10	0.46	9
	BAlb	58–85	2	1.57	415	4	23	32	18	9	5	10	7.26	3.41	0.43	8
	fAhBl	85–106	0	0.78	116	4	20	28	18	10	7	13	6.86	4.37	0.41	11

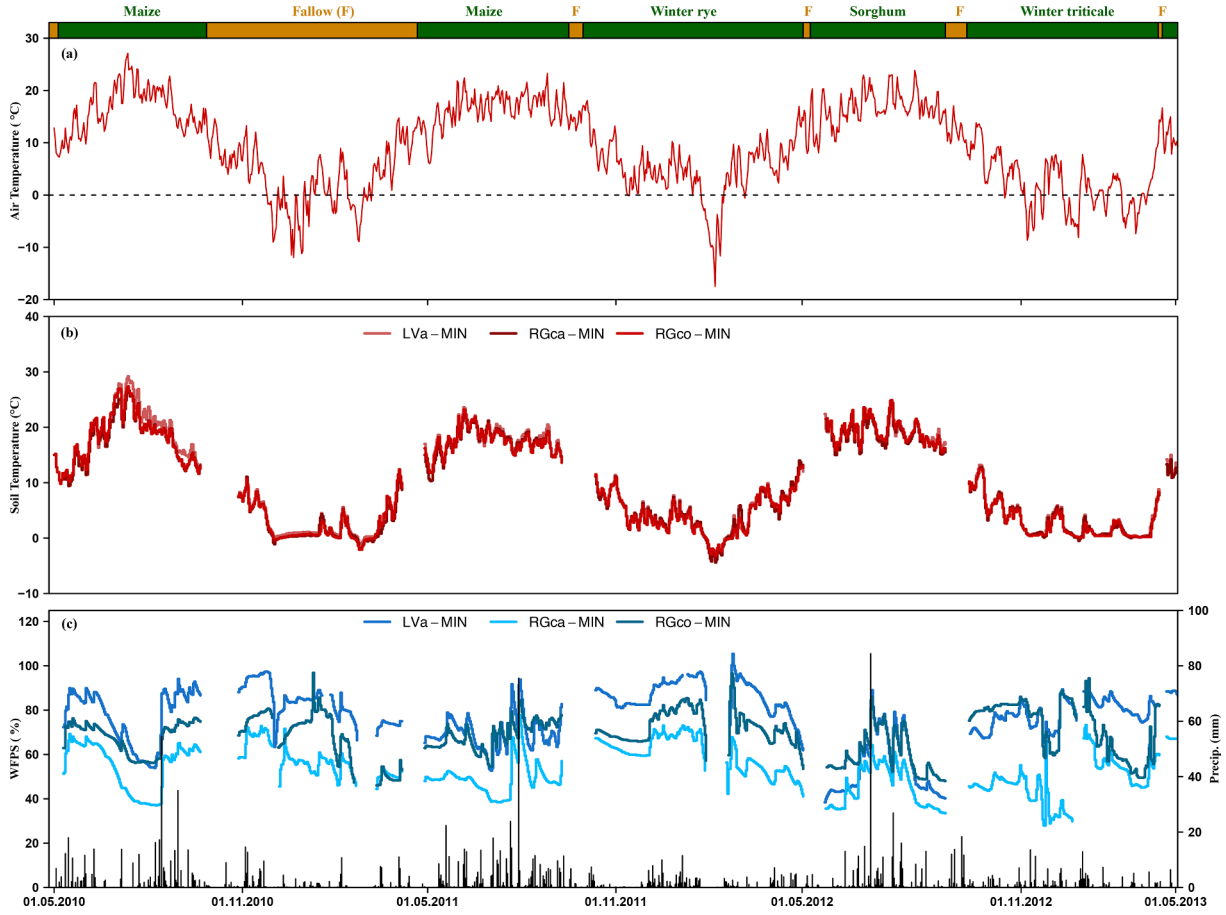

Fig. 2. Environmental conditions at the study area throughout the study period. The panels show a) daily mean air temperature (continuous line), b) soil temperature at 15 cm depth and c) water-filled pore space (WFPS %) and sum daily precipitation (mm d^{-1}) for three distinct erosion states recorded at the climate station, CarboZALF, Dedelow. The abbreviation LVa-MIN, RGca-MIN and RGco-MIN represent three distinct erosion states [Albic Luvisols (LVa; non-eroded soil on flat hilltops), Calcaric Regosols (RGca; extremely eroded soil on steep slopes) and Endogleyic Colluvic Regosols (RGco; depositional soil on depression)] which were mineral fertilized only. The upper coloured region shows the crop rotation during the study period, which includes: Maize (Zea mays L.) – Maize (Zea mays L.) – Winter rye (Secale cereale L.) – Sorghum (Sorghum bicolor) – Triticale (Triticosecale).

Soil temperature recorded at 15 cm soil depth (Fig. 2b) showed a distinct seasonal variation but did not vary significantly between the soil erosion states ($p > 0.05$; Wilcoxon rank-sum test). WFPS, however, evidenced significant differences (15 cm soil depth) between the three soil erosion states ($p < 0.05$; Wilcoxon rank-sum test). With the highest mean WFPS in the LVa-MIN (77.5 %), followed by the RGco-MIN (68.7 %) and the lowest in the RGca-MIN (53.0 %). An increase in %WFPS at all three sites was generally observed following precipitation and freeze–thaw events during winter (Fig. 2c). Three heavy-precipitation events (>50 mm d^{-1}) occurred on 14th August 2010, 29th July 2011 and 7th July 2012.

3.2. Impact of the erosion states on soil properties

The site-specific differences in soil physical and chemical properties for the three distinct erosion states are presented in Table 1. The SOC

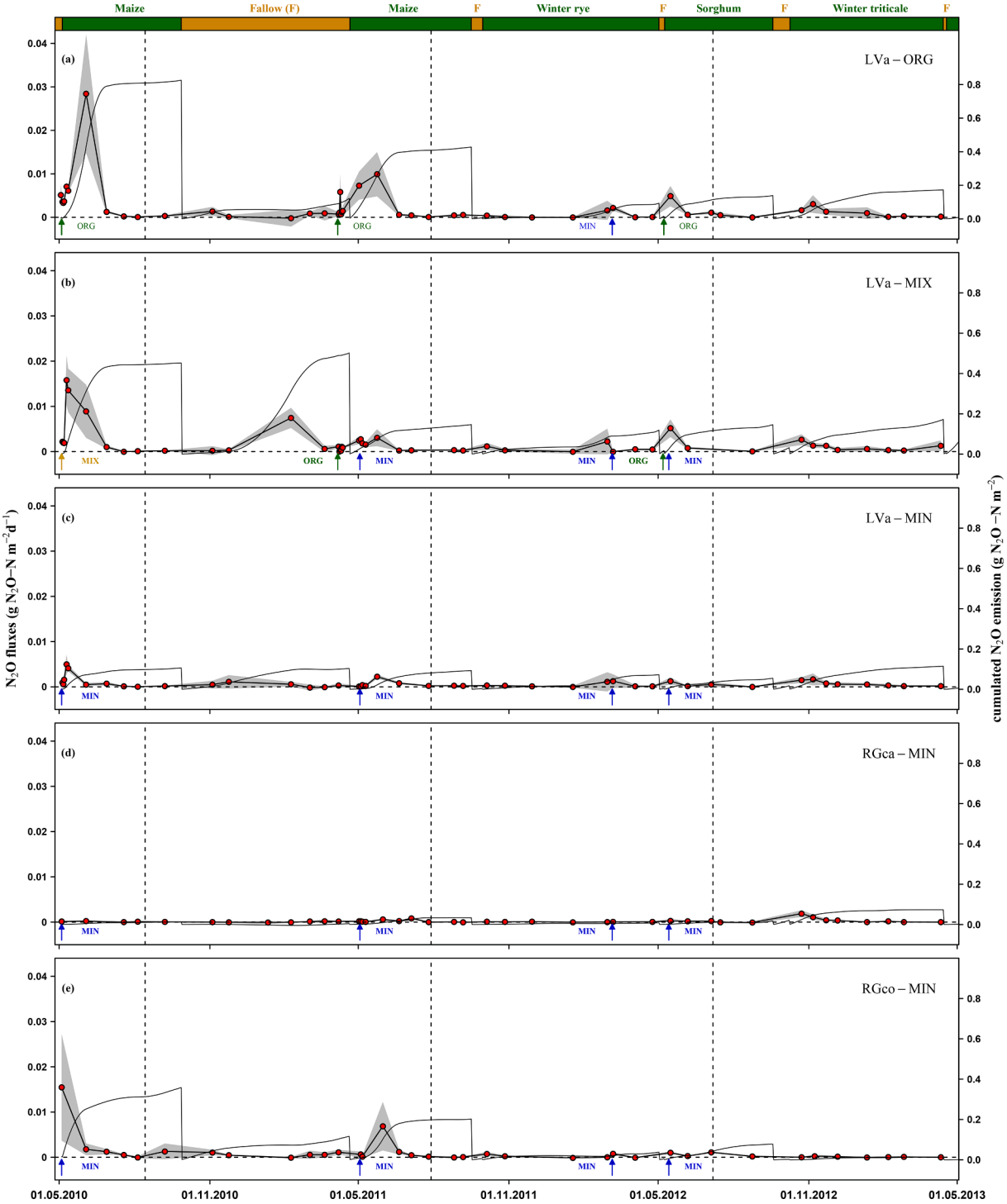

Fig. 3. Temporal dynamics (a-e) of measured (red dots) and interpolated daily N_2O fluxes (left, y-axis) and development of cumulative N_2O fluxes (right, y-axis) measured at the five different measurement sites during the study period (May 2010 to May 2013). The vertical dotted line represents three major precipitation events. Vertical arrows represent the date and type of fertilizers (ORG, MIX, and MIN) (described in Table A2). Sowing of Maize for RGco was done earlier (23.04.2010) than the other sites (05.05.2010). The grey shaded areas show the two-sided error margin (95% confidence interval).

and N_t stocks at the topsoil horizon varied depending on the state of erosion. The highest SOC (18.7 kg m^{-2}) and N_t (2.1 kg m^{-2}) stocks were observed in RGco than LVa and RGca, with greater differences between RGco and RGca. The soil pH increases with depth at all erosion states, except at RGco, which decreases at the deeper depth. At the topsoil horizon, the pH is slightly acidic for RGco (6.31), moderately acidic for LVa (5.53) however, slightly basic for RGca (7.62). The total % sand content is slightly higher for RGca (63 %) compared to LVa (59 %) and RGco (59 %).

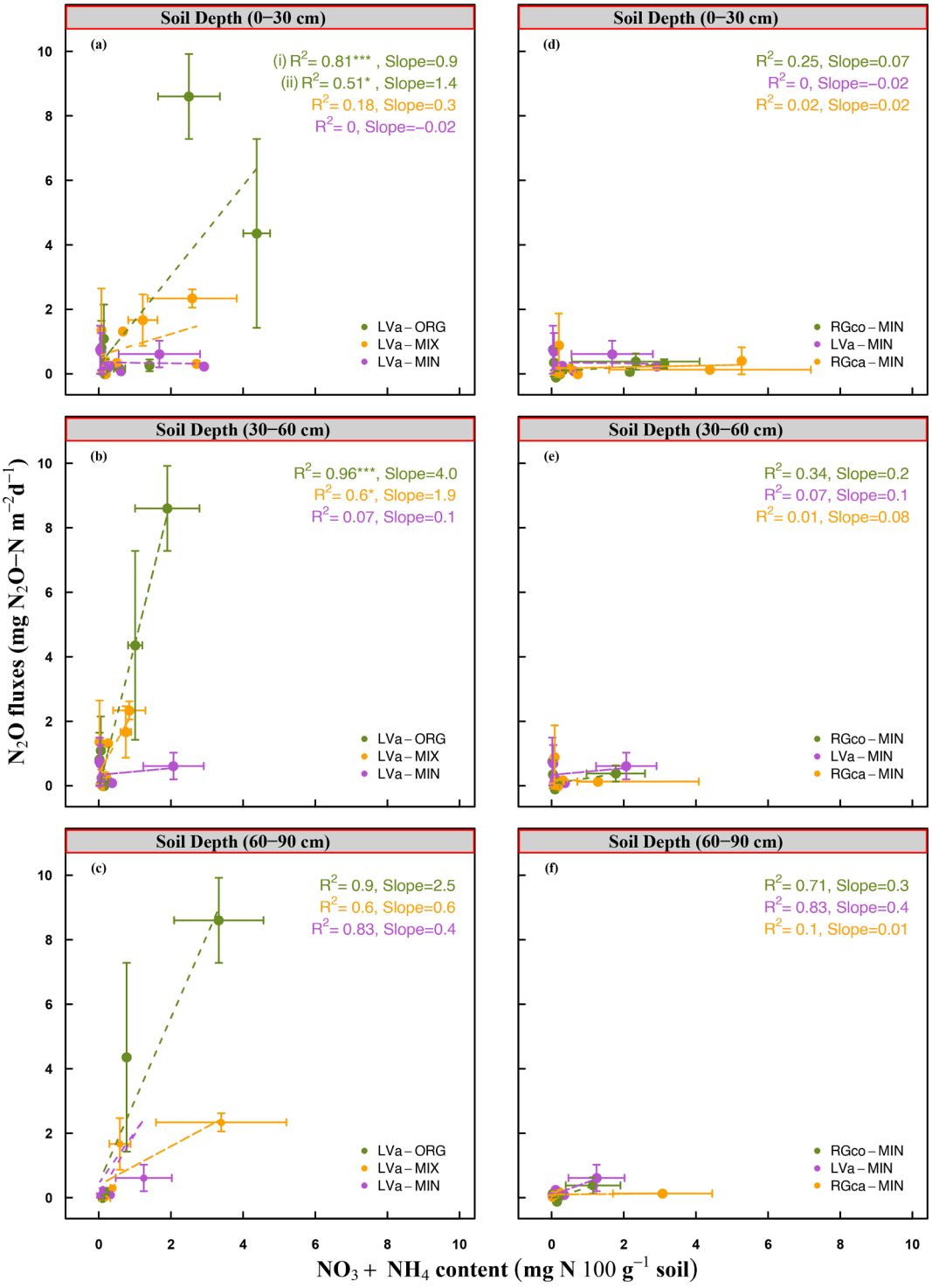

Fig. 4. Relationship between mineral N ($NO_3 + NH_4$) availability at different soil depths (0–30 cm; 30–60 cm and 60–90 cm) and N_2O fluxes. a), b) and c) within the same soil erosion state but with different N fertilizer forms (LVa-ORG, LVa-MIX, LVa-MIN) and d), e) and f) within distinct soil erosion states (RGco-MIN, LVa-MIN, RGca-MIN). The N_2O fluxes were averaged between the two consecutive soil mineral N sampling dates. The dashed lines represent the respective linear regression fit. R^2 and regression slope are given within each plot, following the color scheme of the regression lines. In the case of significant linear regression with leverage and influential data points, R^2 and slope of the linear regression excluding identified influential data points are given in addition. In Fig. 4a, (i) and (ii) indicate R^2 and slope without and with influential data points respectively. For identifying influential data points, the Cook's distance was used. Asterisks (*) indicate the level of significance where, $p < 0.05$ *, $p < 0.01$ ** and $p < 0.001$ ***. The error bars show ± standard error.

3.3. Measured N_2O fluxes

N fertilizer forms significantly influenced measured N_2O fluxes within the same soil erosion state (Fig. 3a-c, F = 5.871, $p = 0.004$, ANOVA). Multiple comparisons suggested that the N_2O fluxes at LVa-ORG and LVa-MIX were significantly higher than at LVa-MIN ($p < 0.05$, ANOVA). However, differences in N_2O fluxes between LVa-ORG and LVa-MIX were not significant ($p = 0.990$, ANOVA). Besides N fertilizer form, distinct soil erosion states also influenced measured N_2O fluxes significantly (Fig. 3c-e, F = 6.572, $p = 0.002$, ANOVA). Multiple comparisons suggested that the N_2O fluxes for the RGco-MIN and LVa-MIN were significantly higher than the RGca-MIN ($p < 0.05$, ANOVA). However, the N_2O fluxes at the RGco-MIN site were not significantly higher than at the LVa-MIN site ($p = 0.883$, ANOVA).

These differences in N_2O fluxes among the N fertilizer forms and distinct soil erosion states were mainly visible in the short term N_2O flux peaks after each N fertilization event at the beginning of the growing season. Further, the N_2O flux peaks in 2010 at all sites were higher than the range of flux peaks measured during the remaining study period except for RGca-MIN. Thus, significant inter annual variability in N_2O fluxes ($F = 6.064$, $p < 0.0006$, ANOVA) within all measured sites was observed (Fig. 3a-e), with the multiple comparisons suggesting that the N_2O fluxes in 2010 were significantly higher for all sites than those measured in 2011, 2012 and 2013 ($p < 0.05$, ANOVA).

Despite a similar N fertilizer amount [152.61 kg N ha^{-1} (ORG)] during the second maize cropping period in 2011, the flux peak was lower compared to the peak observed in 2010 for LVa-ORG. This lower N_2O flux peak in 2011 was accompanied by, in general, lower %WFPS (76 %) but similar air (14.8 °C) and soil temperatures compared to 2010. During the sorghum cropping period in 2012, we observed a lower N_2O flux peak than for maize in 2010 and 2011 for LVa-ORG. This lower flux peak was again accompanied by lower %WFPS and air temperature in 2012 than in 2010 and 2011 (Fig. 2a,c Table A3). In 2012, we observed almost identical N_2O flux peak sizes for LVa-ORG and LVa-MIX but not for LVa-MIN after the application of fertilizers. Although N_2O fluxes were generally low in the fallow period, we observed an exceptional flux peak in LVa-MIX before applying N fertilizer on 8th February 2011 (Fig. 3b). Among the distinct soil erosion states, we observed a higher N_2O flux peak for RGco-MIN compared to LVa-MIN and RGca-MIN during the first maize cropping period of 2010 (Fig. 3c-e). This higher flux peak was observed within a month after applying mineral fertilizers and after that, the flux decreased again. Correspondingly, the highest flux peak obtained in 2010 in LVa-MIN compared to the entire study period was three times lower than the peak in RGco-MIN. In contrast, the RGca-MIN showed low responses to fertilizers and the fluxes remained consistently very low for the entire study period (Fig. 3d). Apart from temperature and %WFPS, LVa-ORG showed a significant correlation between soil mineral N and N_2O fluxes at both the 0–30 cm and the 30–60 cm depth (Fig. 4). However, the relation between soil mineral N and N_2O fluxes for LVa-MIN, RGca-MIN and RGco-MIN was not significant.

3.4. Impact of soil erosion state and N fertilization on aboveground dry matter yield and N removal

On the non-eroded soil, N fertilizer form had no clear effect on aboveground dry matter yield and N uptake. In contrast, the erosion status factor had a clear effect. The two erosion-influenced sites had lower average yields and N uptake compared to the non-eroded soil. The extremely eroded soil (RGca) was the most affected. The difference between the amount of N fertilizer applied and the amount of N taken up by the plants for the entire study period showed negative values, i.e. part of the N taken up originated in the soil's N stock (Table A4).

3.5. Cumulative N_2O emission

The N fertilizer forms, distinct soil erosion states and year strongly affected cumulative N_2O emissions (Fig. 5) and EF (Table 2). We observed higher cumulative N_2O emission during maize 2010 for all sites (except for RGca-MIN) ranging from 1.1 kg N_2O-N ha^{-1} y^{-1} to 8.3 kg N_2O-N ha^{-1} y^{-1} compared to maize 2011 (0.9 to 4.3 kg N_2O-N ha^{-1} y^{-1}) and sorghum 2012 (0.6 to1.5 kg N_2O-N ha^{-1} y^{-1}).

Among the three N fertilizer forms within the same soil erosion state, LVa-ORG showed the highest cumulative N_2O emission (6.2 ± 0.21 kg N_2O-N ha^{-1} y^{-1}) compared to LVa-MIX (5.5 ± 0.18 kg N_2O-N ha^{-1} y^{-1}) and LVa-MIN (1.9 ± 0.17 kg N_2O-N ha^{-1} y^{-1}) (Fig. 5). While comparing the three different soil erosion states, the cumulative N_2O emission at the RGco-MIN (2.8 ± 0.21 kg N_2O-N ha^{-1} y^{-1}) was five times higher than at RGca-MIN (0.6 ± 0.03 kg N_2O-N ha^{-1} y^{-1}) irrespective of the identical mineral fertilizer application. For both LVa-ORG and RGco-MIN which have the highest cumulative N_2O emission, the maize and sorghum contributed 75 % and 76 % to the total cumulative emissions, respectively. In contrast, for LVa-MIX, LVa-MIN and RGca-MIN, the contribution of maize and sorghum was lower than 50 % to the total cumulative N_2O emission (Fig. 5). Likewise, we observed higher EF during the year 2010 for all sites (except for RGca-MIN) varying from 0.7 % to 3.9 % of the total applied N fertilizer compared to maize 2011 (0.6 % to 2.0 %) and sorghum 2012 (0.6 to 1.1 %).

4. Discussion

Our results show that the sites significantly influenced N_2O fluxes, suggesting that both N fertilizer form and erosion state affect cumulative annual N_2O emissions in similar eroded arable croplands. Although the major part of the annual emission was directly linked with the obtained N_2O flux peaks after fertilizer applications, the magnitude of these flux peaks varied among the fertilizer forms and soil erosion states.

Nitrous oxide flux peaks obtained at all measured sites after the application of N fertilizer are in agreement with findings of numerous previous studies (De Rosa et al., 2018; Deng et al., 2017; Skinner et al., 2019; Song et al., 2020). These peaks were caused by applying N fertilizer before or during initial crop growth and thus at a time of low plant N demand, creating favorable conditions for microbial activities, i.e. an increased supply of easily metabolizable *N*-compounds, higher % WFPS and increasing temperature, resulting in higher nitrification and denitrification. It is well known that such conditions can strongly stimulate N_2O formation by nitrifying and denitrifying microorganisms (Bateman and Baggs, 2005; Dai et al., 2020; Dobbie and Smith, 2003; Pareja-Sánchez et al., 2020). The highest N_2O flux peak was observed in 2010 (maize) at all sites (except for extremely eroded soil) and corresponded well with elevated temperature and a %WFPS higher than 60 % during that year's fertilization period (Fig. 3a-e; Table A3). This dependency of N_2O flux peak on %WFPS at all sites was further substantiated by lower flux peaks, observed in 2012 (sorghum), coinciding with a %WFPS <60 % (Fig. A1). A number of studies showed the relationship between WFPS and N_2O emission (Ariani et al., 2021; Dobbie and Smith, 2003; Ruser et al., 2006) as well as confirmed a threshold of 60 % WFPS, above which the N_2O emission increases rapidly after N fertilizer application (Davidson, 1993; Jäger et al., 2011; Jamali et al., 2016; Niu et al., 2018).

Nitrous oxide fluxes from the sites receiving ORG and MIX fertilizer application were significantly higher than from sites receiving MIN fertilizer application within the non-eroded soil. This finding agrees with other studies where higher N_2O flux peaks were observed after organic fertilizer application compared to mineral fertilizer application (Van Groenigen et al., 2004; Velthof and Rietra, 2018; Zhou et al., 2017). Differences between N_2O fluxes of mineral and organic fertilizer were generally found on coarse textured soil than in fine textured soil. On the one hand, Han et al. (2017) argued that this could be due to the limitation of soil C availability usually present in the coarse textured soil, which might limit denitrification. On the other hand, there is more

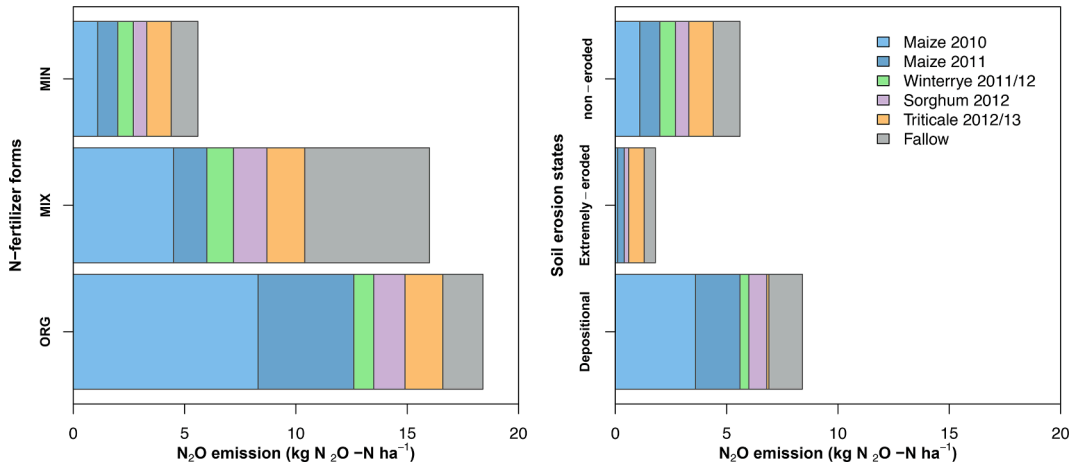

Fig. 5. Stacked bar diagram showing cumulative N_2O emissions combining measurements of all three years with (left) three different N fertilizer forms: ORG, MIN and MIX representing organic, mineral and mixture of organic and mineral fertilizer forms, respectively applied at non-eroded soil (LVa) and (right) three different soil erosion states [Albic Cutanic Luvisol (LVa; non-eroded soil), Calcaric Regosol (RGca; extremely eroded soil), Endogleyic Colluvic Regosol (RGco; depositional soil)] with same N fertilizer form (MIN).

Table 2
Cumulative N_2O emission of maize 2010, maize 2011 and sorghum 2012 as affected by the total nitrogen fertilizer (kg N/ha) applied at the five measurement sites Given ± refers to the calculated uncertainty estimate of annual N_2O emissions following the approach of Huth et al. (2018).

Year	Temperature (AVG)	Precipitation (SUM)	WFPS (AVG)	Crop type	Site	Applied N_t Fertilizer (kg N ha^{-1})	Cumulative emission (kg N_2O-N ha^{-1})	Emission Factor (%)
2010	11.2	469.7	83	Maize	LVa-ORG	213.7	8.3 ± 0.5	3.9
			NA	Maize	LVa-MIX	219.4	4.5 ± 0.3	2.1
			77	Maize	LVa-MIN	160	1.1 ± 0.1	0.7
			55	Maize	RGca-MIN	160	0.1 ± 0.02	0.1
			68	Maize	RGco-MIN	160	3.6 ± 0.5	2.2
2011	10.0	618.1	75	Maize	LVa-ORG	218	4.3 ± 0.3	2.0
			NA	Maize	LVa-MIX	179.2	1.5 ± 0.1	0.8
			70	Maize	LVa-MIN	160	0.9 ± 0.03	0.6
			49	Maize	RGca-MIN	160	0.3 ± 0.02	0.2
			69	Maize	RGco-MIN	160	2.0 ± 0.2	1.3
2012	9.3	584.4	64	Sorghum	LVa-ORG	141	1.4 ± 0.1	1.0
			NA	Sorghum	LVa-MIX	129.1	1.5 ± 0.1	1.1
			55	Sorghum	LVa-MIN	100	0.6 ± 0.1	0.6
			45	Sorghum	RGca-MIN	100	0.2 ± 0.1	0.2
			60	Sorghum	RGco-MIN	100	0.8 ± 0.03	0.8

labile C in clay-rich soils from the outset, therefore the N_2O production and emission should be even higher here. Hence it is much more likely that in sandy soils, due to the lack of reactive clay surfaces, more labile C/N compounds are exposed to direct microbial access, i.e., are rapidly and more extensively mineralized (Islam and Singh, 2022). In general, the higher N_2O fluxes in ORG fertilized soil than MIN fertilized soil can be likely attributed to the substantial increase in the supply of microbially easily accessible C- and *N*-compounds through organic fertilizer application. Adding additional C and N through ORG fertilization might enhance microbial activity leading to the consumption of O_2, hence creating anoxic conditions in the soil due to O_2 depletion, which further promotes denitrification and enhances N_2O fluxes (O'Neill et al., 2020). The significant correlation between soil mineral N and N_2O flux at ORG indicates that (Fig. 4). However, as the results of the analyses also show, these relationships can also change significantly even at short distances due to erosion. Of course, it is also conceivable that these relationships are subject to strong temporal dynamics. This is especially true for depositional soils, because anaerobic conditions can develop very quickly here, even without the addition of readily degradable C and N compounds, due to the rise of groundwater. Hence, subsequent process studies are required to clarify this conclusively.

We also observed N_2O emissions peaked at most sites in late 2012, although no fertilizers were applied. These peaks can be related to a changing % WFPS due to frequent precipitation events and reduced evapotranspiration at low temperature (Fig. 2c). In addition to that, multiple studies showed that freeze–thaw events result in enhanced N_2O fluxes (Chen et al., 2019; McGowan et al., 2019; Song et al., 2017; Weller et al., 2019) through soil O_2 depletion as a result of enhanced microbial respiration (Mørkved et al., 2006) and stimulation of N_2O production via denitrification. This might help to explain the minor peak in N_2O fluxes, obtained during late February 2012 at all sites, since enhanced N_2O fluxes directly followed a thawing period after almost one month of

continuously frozen soil (Fig. 2).

The cumulative N_2O emissions obtained in this study at all five sites (Table. 2) were within the range of values derived from field experiments within Germany and summarized by Jungkunst et al. (2006). In line with the study of Kaiser et al. (2000), which investigated arable soils across Germany, the N_2O emissions obtained in our study were higher in the ORG fertilized site (6.2 kg N_2O-N ha^{-1} y^{-1}) compared to the MIN fertilized site (0.6 kg N_2O-N ha^{-1} y^{-1}) while the MIX variant was in between but closer to the ORG variant (5.5 kg N_2O-N ha^{-1} y^{-1}). These differences in cumulative N_2O emission values resulted primarily from the differences in the N_2O flux peaks after the application of N fertilizer. Thus, both the results on current N_2O fluxes and those on cumulative annual N_2O emissions confirmed our first hypothesis, that in the non-eroded soil, N_2O fluxes are higher from ORG and MIX fertilized soil compared to MIN fertilized soil. In agreement with our second hypothesis, our result showed that erosion state had a similarly strong impact on N_2O fluxes and thereby cumulative emission as N fertilizer form. This finding is similar to the previous landscape-scale study by Vilain et al. (2010), which found more than three times higher N_2O emissions in depositional soil than at a slope and summit position. Also, Gu et al. (2011) reported higher N_2O emission in depositional soil compared to the summit, but only for one of their three study sites, which was characterized by comparable pH and soil moisture content when compared to our study sites.

Depending on the erosion state, we observed distinct site-specific differences in soil physical and chemical properties (Fig. 2c, Table 1), which might have influenced the N_2O emissions (Fig. 3c-e). The higher N_2O fluxes in depositional soil might be associated with the observed higher SOC and N_t contents compared to non-eroded and extremely eroded soil. A similar positive correlation between N_2O emission and SOC content was observed by Stehfest and Bouwman (2006), analyzing data from 1008 N_2O emission measurements from agricultural soils. Similar to this study, higher SOC and N_t contents in depositional soil than other slope positions were confirmed by numerous previous studies. In addition to the higher SOC and N_t stocks in the depositional soil, the higher groundwater level and a topsoil WFPS, almost continuously >60 % (Fig. 2c), might have created favorable conditions for denitrification, enhancing N_2O fluxes compared to the extremely eroded soil. The higher N_2O emission with increasing moisture content in the depositional soil was also found by Ashiq et al. (2021) and Gu et al. (2013), identifying soil moisture as one of the factors driving N_2O emission in erosion affected arable croplands. This further emphasizes the effect of a WFPS >60 % on N_2O emissions.

The study area generally has a sandy soil texture. The lower fluxes observed at extremely eroded soil might be caused by a higher sand content (64 %) on the topsoil, enabling good soil aeration through the macropores compared to deposited and non-eroded soil. The higher sand content decreases the soil water-holding capacity and %WFPS (Li et al., 2018; Ruser et al., 2017), which also tends to be the case for the extremely eroded soil (Fig. 2c), creating less favorable conditions for nitrification and denitrification. Jamali et al. (2016) reported decreasing N_2O fluxes with increasing sand content in a lysimeter study concerning the effect of soil texture on N_2O fluxes. Although we observed higher mineral N concentrations at 0–30 cm soil depth for the extremely eroded soil (Fig. 4), N_2O fluxes remained low, which might be because of lower %WFPS (Fig. 2c) as well as lower availability of labile C (lower SOC content; Table 1), both might limit denitrification.

The soil pH has been identified as another main regulator of soil N_2O fluxes (Hénault et al., 2019; Jamali et al., 2016; Stehfest and Bouwman, 2006), affecting microbial community composition and activity in the soil. In acidic conditions, it is generally believed that the size of a nitrifying and denitrifying community is smaller (Jadeja et al., 2021; Park et al., 2018; Šimek et al., 2002), and therefore, the production of N_2O is lower. Thus, the moderately acidic conditions observed in LVa-MIN (pH = 5.5) might have inhibited the nitrification and denitrification process despite the higher %WFPS and thus lowered the N_2O flux compared to RGco-MIN.

The slightly alkaline conditions at the extremely eroded soil might be responsible for the observed low N_2O emissions (Stehfest and Bouwman, 2006). However, studies which estimated both N_2O and N_2 emission showed that in highly fertilized soils such as croplands, N_2O:($N_2O + N_2$) emission ratio and N_2O emissions might also increase with decreasing pH (Qu et al., 2014). This is explained by the suppression of N_2O reductase, which inhibits the reduction of N_2O to N_2, yielding in an incomplete denitrification (Pan et al., 2022; Senbayram et al., 2012).

To determine whether the discussed factor constellations are indeed responsible for the strong effect of the erosion state on N_2O emissions, subsequent investigations are required to understand how they interact with the processes responsible for N_2O formation, turnover and transport. The higher N uptake, compared to N fertilizer application, for all variants suggests that excess fertilizer N, probably did not contribute to the differences in N_2O emissions. This is much more likely due to erosion-related differences in soil N stocks, as already indicated. This may be accompanied by differences in N mineralization, which simultaneously provide soluble N compounds for N uptake by plants as well as for N_2O formation. However, clear statements on this are only possible on the basis of inter-alia 15 N isotope studies. Furthermore, annual N_2O emission estimates, which might be highly affected by erratic short-term emission events, could be further improved through inter-alia enhancing the measurement frequency. As suggested by Grace et al. (2020) and Barton et al. (2015), especially automatic, continuous measurement systems might better reflect the temporal dynamics of N_2O emissions throughout the year. At the same time, however, these systems still need to allow for multiple nearby treatment comparisons and spatial repetitions.

5. Conclusion

Our results demonstrated that N_2O emissions of heterogeneous cropland were influenced not only by N fertilizer forms but to a similar degree also by the soil erosion states. While higher cumulative N_2O emissions were observed at the site with organic fertilization compared to mineral fertilizer and a mix of organic and mineral fertilizers, the depositional soil showed higher N_2O emissions compared to the eroded and non-eroded soil. These higher emissions were mainly explained by site-specific differences in soil properties and soil water content, which might be attributed to terrain position and soil erosion. To determine possible interactions and the impact of these two strong factors on N_2O emissions or overall N dynamics of eroded croplands, it is necessary to perform additional, replicated, multi-factorial experiments testing a wide range of combinations of erosion states, N fertilizer rates and forms. It is likely that with reduced N fertilizer application, the erosion state will increasingly influence N_2O emission in two ways: Firstly, as a result of differences in soil N stocks caused by erosion or deposition (Table 1); and secondly, as a result of the differences in the soil air balance of the non-eroded and the heavily eroded soil (primarily aerobic) and the depositional soil (often anaerobic) (Fig. 1). Based on such studies, it will be possible to develop measures for more effective use of N fertilization and N_2O emission reduction on eroded cropland.

Data availability statements

The data that support the findings of this study are openly available through the ZALF open-research-data repository at https://doi.org/10.4228/zalf.byaf-7748.

Declaration of Competing Interest

The authors declare that they have no known competing financial interests or personal relationships that could have appeared to influence the work reported in this paper.

Data availability

The link to the data is provided in the manuscript.

Acknowledgements

This study was supported by the German Federal Ministry of Food and Agriculture (FNR Grant: 22404117) within the research project "Krumensenke." The authors are very grateful to all the employees of the ZALF who supported during field measurements campaigns and the laboratory analyses.

Appendix A. Supplementary data

Supplementary data to this article can be found online at https://doi.org/10.1016/j.geoderma.2022.116243.

References

Ariani, M., Setyanto, P., Wihardjaka, A., 2021. Water filled-pore space and soil temperature related to N_2O fluxes from shallot cultivated in rainy and dry season. IOP Conf. Ser. Earth Environ. Sci. 648 (1), 012109.

Ashiq, W., Vasava, H.B., Ghimire, U., Daggupati, P., Biswas, A., 2021. Topography controls N_2O emissions differently during early and late corn growing season. Agronomy 11, 1–19. https://doi.org/10.3390/agronomy11010187.

Barton, L., Kiese, R., Gatter, D., Butterbach-bahl, K., Buck, R., Hinz, C., Murphy, D.V., 2008. Nitrous oxide emissions from a cropped soil in a semi-arid climate. Glob. Chang. Biol. 14, 177–192. https://doi.org/10.1111/j.1365-2486.2007.01474.x.

Barton, L., Wolf, B., Rowlings, D., Scheer, C., Kiese, R., Grace, P., Stefanova, K., Butterbach-Bahl, K., 2015. Sampling frequency affects estimates of annual nitrous oxide fluxes. Nat. Publ. Gr. 5 (1) https://doi.org/10.1038/srep15912.

Bateman, E.J., Baggs, E.M., 2005. Contributions of nitrification and denitrification to N_2O emissions from soils at different water-filled pore space. Biol. Fertil. Soils 41, 379–388. https://doi.org/10.1007/s00374-005-0858-3.

Berhe, A.A., Barnes, R.T., Six, J., Marín-Spiotta, E., 2018. Role of Soil Erosion in Biogeochemical Cycling of Essential Elements: Carbon, Nitrogen, and Phosphorus. Annu. Rev. Earth Planet. Sci. 46, 521–548. https://doi.org/10.1146/annurev-earth-082517-010018.

Bouwman, A.F., Boumans, L.J.M., Batjes, N.H., 2002. Emissions of N_2O and NO from fertilized fields: Summary of available measurement data. Global Biogeochem. Cycles 16 (4), 6-1–6-13.

Buchen-Tschiskale, C., Hagemann, U., Augustin, J., 2020. Soil incubation study showed biogas digestate to cause higher and more variable short-term N_2O and N_2 fluxes than mineral-N. J. Plant Nutr. Soil Sci. 183 (2), 208–219.

Chen, W., Zheng, X., Wolf, B., Yao, Z., Liu, C., Butterbach-Bahl, K., Brüggemann, N., 2019. Long-term grazing effects on soil-atmosphere exchanges of CO_2, CH_4 and N_2O at different grasslands in Inner Mongolia: A soil core study. Ecol. Indic. 105, 316–328. https://doi.org/10.1016/j.ecolind.2017.09.035.

Ciais, P., Sabine, C., Bala, G., Bopp, L., Brovkin, V., Canadell, J., Chhabra, A., DeFries, R., Galloway, J., Heimann, M., Jones, C., Quéré, C.L., Myneni, R.B., Piao, S., Thornton, P., 2013. The physical science basis. Contribution of working group I to the fifth assessment report of the intergovernmental panel on climate change, In Climate Change. https://doi.org/10.1017/CBO9781107415324.015.

Corre, M.D., van Kessel, C., Pennock, D.J., 1996. Landscape and Seasonal Patterns of Nitrous Oxide Emissions in a Semiarid Region. Soil Sci. Soc. Am. J. 60, 1806–1815. https://doi.org/10.2136/sssaj1996.03615995006000060028x.

Dai, Z., Yu, M., Chen, H., Zhao, H., Huang, Y., Su, W., Xia, F., Chang, S.X., Brookes, P.C., Dahlgren, R.A., Xu, J., 2020. Elevated temperature shifts soil N cycling from microbial immobilization to enhanced mineralization, nitrification and denitrification across global terrestrial ecosystems. Glob. Chang. Biol. 26, 5267–5276. https://doi.org/10.1111/gcb.15211.

Davidson, E.A., 1993. Soil Water Content and the Ratio of Nitrous Oxide to Nitric Oxide Emitted from Soil. Biogeochem. Glob. Chang. 369–386 https://doi.org/10.1007/978-1-4615-2812-8_20.

De Rosa, D., Rowlings, D.W., Biala, J., Scheer, C., Basso, B., Grace, P.R., 2018. N_2O and CO_2 emissions following repeated application of organic and mineral N fertiliser from a vegetable crop rotation. Sci. Total Environ. 637–638, 813–824. https://doi.org/10.1016/j.scitotenv.2018.05.046.

Deng, M., Hou, M., Ohtsu, N.O., Yokoyama, T., Tanaka, H., Nakajima, K., Omata, R., Dorothea, S., Kimura, B., 2017. Nitrous Oxide Emission from Organic Fertilizer and Controlled Release Fertilizer in Tea Fields. Agriculture 1–12. https://doi.org/10.3390/agriculture7030029.

DIN ISO 10694, 1996. Bodenbeschaffenheit:Bestimmungvon organischem Kohlenstoffund Gesamtkohlenstoff nach trockener Verbrennung (Elementaranalyse). Berlin.

Dobbie, K.E., Smith, K.A., 2003. Nitrous oxide emission factors for agricultural soils in Great Britain: The impact of soil water-filled pore space and other controlling variables. Glob. Chang. Biol. 9, 204–218. https://doi.org/10.1046/j.1365-2486.2003.00563.x.

Doetterl, S., Berhe, A.A., Nadeu, E., Wang, Z., Sommer, M., Fiener, P., 2016. Erosion, deposition and soil carbon: A review of process-level controls, experimental tools and models to address C cycling in dynamic landscapes. Earth-Science Rev. 154, 102–122. https://doi.org/10.1016/j.earscirev.2015.12.005.

Forrestal, P.J., Adani, I., Snauwaert, E., Veeken, A., Bernard, J., Jensen, L.S., 2016. EIP-AGRI Focus Group - Nutrient recycling Mini-paper - Towards increasing the mineral fertiliser replacement value of bio-based fertilisers Authors 21.

Gelfand, I., Shcherbak, I., Millar, N., Kravchenko, A.N., Robertson, G.P., 2016. Long-term nitrous oxide fluxes in annual and perennial agricultural and unmanaged ecosystems in the upper Midwest USA. Glob. Chang. Biol. 22, 3594–3607. https://doi.org/10.1111/gcb.13426.

Grace, P.R., Weerden, T.J., Rowlings, D.W., Scheer, C., Brunk, C., Kiese, R., Butterbach-Bahl, K., Rees, R.M., Robertson, G.P., Skiba, U.M., 2020. Global Research Alliance N_2O chamber methodology guidelines: Considerations for automated flux measurement. J. Environ. Qual. 49 (5), 1126–1140.

Gu, J., Nicoullaud, B., Rochette, P., Pennock, D.J., Hénault, C., Cellier, P., Richard, G., 2011. Effect of topography on nitrous oxide emissions from winter wheat fields in Central France. Environ. Pollut. 159, 3149–3155. https://doi.org/10.1016/j.envpol.2011.04.009.

Gu, J., Nicoullaud, B., Rochette, P., Grossel, A., Hénault, C., Cellier, P., Richard, G., 2013. A regional experiment suggests that soil texture is a major control of N_2O emissions from tile-drained winter wheat fields during the fertilization period. Soil Biol. Biochem. 60, 134–141. https://doi.org/10.1016/j.soilbio.2013.01.029.

Han, Z., Walter, M.T., Drinkwater, L.E., 2017. Impact of cover cropping and landscape positions on nitrous oxide emissions in northeastern US agroecosystems. Agric. Ecosyst. Environ. 245, 124–134. https://doi.org/10.1016/j.agee.2017.05.018.

Hénault, C., Bourennane, H., Ayzac, A., Ratié, C., Saby, N.P.A., Cohan, J.-P., Eglin, T., Gall, C.L., 2019. Management of soil pH promotes nitrous oxide reduction and thus mitigates soil emissions of this greenhouse gas. Scientific Reports 9 (1). https://doi.org/10.1038/s41598-019-56694-3.

Hoffmann, M., Jurisch, N., Alba, J., Borraz, E., Schmidt, M., Huth, V., Rogasik, H., Rieckh, H., Verch, G., Sommer, M., Augustin, J., 2017. Detecting small-scale spatial heterogeneity and temporal dynamics of soil organic carbon (SOC) stocks: A comparison between automatic chamber-derived C budgets and repeated soil inventories. Biogeosciences 14, 1003–1019. https://doi.org/10.5194/bg-14-1003-2017.

Hoffmann, M., Pehle, N., Huth, V., Jurisch, N., Sommer, M., Augustin, J., 2018a. A simple method to assess the impact of sealing, headspace mixing and pressure vent on airtightness of manually closed chambers. J. Plant Nutr. Soil Sci. 181, 36–40. https://doi.org/10.1002/jpln.201600299.

Hoffmann, M., Pohl, M., Jurisch, N., Prescher, A.K., Mendez Campa, E., Hagemann, U., Remus, R., Verch, G., Sommer, M., Augustin, J., 2018b. Maize carbon dynamics are driven by soil erosion state and plant phenology rather than nitrogen fertilization form. Soil Tillage Res. 175, 255–266. https://doi.org/10.1016/j.still.2017.09.004.

Huang, R., Wang, Y., Gao, X., Liu, J., Wang, Z., Gao, M., 2020. Nitrous oxide emission and the related denitrifier community: A short-term response to organic manure substituting chemical fertilizer. Ecotoxicol. Environ. Saf. 192, 110291 https://doi.org/10.1016/j.ecoenv.2020.110291.

Huth, V., Hoffmann, M., Bereswill, S., Popova, Y., Zak, D., Augustin, J., 2018. The climate warming effect of a fen peat meadow with fluctuating water table is reduced by young alder trees. Mires Peat 21, 1–18. https://doi.org/10.19189/MaP.2017.OMB.291.

IPCC, 2022. Climate Change 2022, Summary for Policymakers. Climate Change 2022: Mitigation of Climate Change. Contribution of Working Group III to the Sixth Assessment Report of the Intergovernmental Panel on Climate Change. UK and New York, NY, USA.

Islam, R., Singh, B., 2022. Stabilisation of soil organic matter : interactions between clay and microbes. Biogeochemistry 160, 145–158. https://doi.org/10.1007/s10533-022-00956-2.

Jadeja, A.S., Hirpara, D.V., Vekaria, L.C., Sakarvadia, H.L., 2021. Soil Fertility and Nutrient Management: [A Way to Sustainable Agriculture], 1st ed. CRC Press.

Jäger, N., Stange, C.F., Ludwig, B., Flessa, H., 2011. Emission rates of N_2O and CO_2 from soils with different organic matter content from three long-term fertilization experiments-a laboratory study. Biol. Fertil. Soils 47, 483–494. https://doi.org/10.1007/s00374-011-0553-5.

Jamali, H., Quayle, W., Scheer, C., Rowlings, D., Baldock, J., 2016. Effect of soil texture and wheat plants on N_2O fluxes: A lysimeter study. Agric. For. Meteorol. 223, 17–29. https://doi.org/10.1016/j.agrformet.2016.03.022.

Jungkunst, H.F., Freibauer, A., Neufeldt, H., Bareth, G., 2006. Nitrous oxide emissions from agricultural land use in Germany - A synthesis of available annual field data. J. Plant Nutr. Soil Sci. 169, 341–351. https://doi.org/10.1002/jpln.200521954.

Jurasinski, G., Koebsch, F., Hagemann, U., Günther, A., 2014. Flux rate calculation from dynamic closed chamber measurements. R package.

Kaiser, E.A., Ruser, R., Munch, J.C., 2000. Nitrous oxide emissions from arable soils in Germany - An evaluation of six long-term field experiments. J. Plant Nutr. Soil Sci. 163, 249–259. https://doi.org/10.1002/1522-2624(200006)163:3<249::aid-jpln249>3.0.co;2-z.

Kong, W., Yao, Y., Hou, L., Bao, K., Zhang, L., Wei, X., 2022. Effects of vegetation presence on soil net N mineralization are independent of landscape position and vegetation type in an eroding watershed. Agric. Ecosyst. Environ. 325, 107743 https://doi.org/10.1016/j.agee.2021.107743.

Kudeyarov, V.N., 2020. Nitrous oxide emission from fertilized soils: an analytical review. Eurasian Soil Sci. 53, 1396–1407. https://doi.org/10.1134/S1064229320100105.

Kumar, P., Lai, L., Battaglia, M.L., Kumar, S., Owens, V., Fike, J., Galbraith, J., Hong, C. O., Farris, R., Crawford, R., Crawford, J., Hansen, J., Mayton, H., Viands, D., 2019. Impacts of nitrogen fertilization rate and landscape position on select soil properties

in switchgrass field at four sites in the USA. Catena 180, 183–193. https://doi.org/10.1016/j.catena.2019.04.028.
Lal, R., 2019. Accelerated Soil erosion as a source of atmospheric CO_2. Soil Tillage Res. 188, 35–40. https://doi.org/10.1016/j.still.2018.02.001.
Lassaletta, L., Billen, G., Garnier, J., Bouwman, L., Velazquez, E., Mueller, N.D., Gerber, J.S., 2016. Nitrogen use in the global food system: Past trends and future trajectories of agronomic performance, pollution, trade, and dietary demand. Environ. Res. Lett. 11 (9), 095007.
Li, X., McCarty, G.W., Lang, M., Ducey, T., Hunt, P., Miller, J., 2018. Topographic and physicochemical controls on soil denitrification in prior converted croplands located on the Delmarva Peninsula, USA. Geoderma 309, 41–49. https://doi.org/10.1016/j.geoderma.2017.09.003.
Li, T., Zhang, H., Wang, X., Cheng, S., Fang, H., Liu, G., Yuan, W., 2019. Soil erosion affects variations of soil organic carbon and soil respiration along a slope in Northeast China. Ecol. Process. 8 https://doi.org/10.1186/s13717-019-0184-6.
Lin, H., Xie, Y., Liu, G., Zhai, J., Li, S., 2019. Soybean and maize simulation under different degrees of soil erosion. F. Crop. Res. 230, 1–10. https://doi.org/10.1016/j.fcr.2018.10.004.
Lind, S.E., Maljanen, M., Hyvönen, N.P., Kutvonen, J., Jokinen, S., Räty, M., Virkajärvi, P., Martikainen, P.J., 2019. Nitrous oxide emissions from perennial grass cropping systems on a boreal mineral soil 2469, 215–232.
Velthof, G., Rietra, R.P.J., 2015. Nitrous oxide emission from agricultural soils. Wageningen Environ. Res. Rep. 7 (1), 62.
Livingston, G.P., Hutchinson, G.L., 1995. Enclosure-based measurement of trace gas exchange: applications and sources of error. In: Matson, P.A., Harris, R.C. (Eds.), Methods in Ecology. Biogenic Trace Gases: Measuring Emissions From Soil and Water. Blackwell Science, Oxford, U.K, pp. 14–51.
Loftfield, N., Flessa, H., Augustin, J., Beese, F., 1997. Automated gas chromatographic system for rapid analysis of the atmospheric trace gases methane. Carbon Dioxide, and Nitrous Oxide 26 (2), 560–564.
Mbonimpa, E.G., Hong, C.O., Owens, V.N., Lehman, R.M., Osborne, S.L., Schumacher, T. E., Clay, D.E., Kumar, S., 2015. Nitrogen fertilizer and landscape position impacts on CO_2 and CH_4 fluxes from a landscape seeded to switchgrass. GCB Bioenergy 7, 836–849. https://doi.org/10.1111/gcbb.12187.
Mbow, C., Rosenzweig, C., Barioni, L.G., Benton, T.G., Herrero, M., Krishnapillai, M., Liwenga, E., Pradhan, P., Rivera-Ferre, M.G., Sapkota, T., Tubiello, F., Xu, Y., 2019. Climate change and land. Chapter 5: Food Security. IPCC Spec. Rep. 1–200.
McGowan, A.R., Roozeboom, K.L., Rice, C.W., 2019. Nitrous oxide emissions from annual and perennial biofuel cropping systems. Agron. J. 111, 84–92. https://doi.org/10.2134/agronj2018.03.0187.
Millar, N., Philip Robertson, G., Grace, P.R., Gehl, R.J., Hoben, J.P., 2010. Nitrogen fertilizer management for nitrous oxide (N_2O) mitigation in intensive corn (Maize) production: An emissions reduction protocol for US Midwest agriculture. Mitig. Adapt. Strateg. Glob. Chang. 57, 185–204. https://doi.org/10.1007/s11027-010-9212-7.
Mørkved, P.T., Dörsch, P., Henriksen, T.M., Bakken, L.R., 2006. N_2O emissions and product ratios of nitrification and denitrification as affected by freezing and thawing. Soil Biol. Biochem. 38, 3411–3420. https://doi.org/10.1016/j.soilbio.2006.05.015.
Navas, A., Gaspar, L., Quijano, L., López-Vicente, M., Machín, J., 2012. Patterns of soil organic carbon and nitrogen in relation to soil movement under different land uses in mountain fields (South Central Pyrenees). Catena 94, 43–52. https://doi.org/10.1016/j.catena.2011.05.012.
Negassa, W., Price, R.F., Basir, A., Snapp, S.S., Kravchenko, A., 2015. Cover crop and tillage systems effect on soil CO_2 and N_2O fluxes in contrasting topographic positions. Soil Tillage Res. 154, 64–74. https://doi.org/10.1016/j.still.2015.06.015.
Nie, X.J., Zhang, H.B., Su, Y.Y., 2019. Soil carbon and nitrogen fraction dynamics affected by tillage erosion. Sci. Rep. 9, 1–8. https://doi.org/10.1038/s41598-019-53077-6.
Niu, Y., Luo, J., Liu, D., Müller, C., Zaman, M., Lindsey, S., Ding, W., 2018. Effect of biochar and nitrapyrin on nitrous oxide and nitric oxide emissions from a sandy loam soil cropped to maize. Biol. Fertil. Soils 54, 645–658. https://doi.org/10.1007/s00374-018-1289-2.
O'Neill, M., Gallego-Lorenzo, L., Lanigan, G.J., Forristal, P.D., Osborne, B.A., 2020. Assessment of nitrous oxide emission factors for arable and grassland ecosystems. J. Integr. Environ. Sci. 00, 1–21. https://doi.org/10.1080/1943815X.2020.1825227.
Pan, B., Xia, L., Lam, S.K., Wang, E., Zhang, Y., Mosier, A., Chen, D., 2022. A global synthesis of soil denitrification: Driving factors and mitigation strategies. Agric. Ecosyst. Environ. 327, 107850 https://doi.org/10.1016/j.agee.2021.107850.
Pareja-Sánchez, E., Cantero-Martínez, C., Álvaro-Fuentes, J., Plaza-Bonilla, D., 2020. Impact of tillage and N fertilization rate on soil N_2O emissions in irrigated maize in a Mediterranean agroecosystem. Agric. Ecosyst. Environ. 287, 106687 https://doi.org/10.1016/j.agee.2019.106687.
Park, S.H., Lee, B.R., Jung, K.H., Kim, T.H., 2018. Acidification of pig slurry effects on ammonia and nitrous oxide emissions, nitrate leaching, and perennial ryegrass regrowth as estimated by 15N-urea flux. Asian-Australasian J. Anim. Sci. 31, 457–466. https://doi.org/10.5713/ajas.17.0556.
Pradhan, P., Fischer, G., van Velthuizen, H., Reusser, D.E., Kropp, J.P., Gonzalez-Andujar, J.L., 2015. Closing yield gaps: How sustainable can we be? PLoS One 10 (6), e0129487.
Prăvălie, R., Patriche, C., Borrelli, P., Panagos, P., Roşca, B., Dumitraşcu, M., Nita, I.-A., Săvulescu, I., Birsan, M.-V., Bandoc, G., 2021. Arable lands under the pressure of multiple land degradation processes. A global perspective. Environ. Res. 194, 110697.
Qu, Z., Wang, J., Almøy, T., Bakken, L.R., 2014. Excessive use of nitrogen in Chinese agriculture results in high $N_2O/(N_2O+N_2)$ product ratio of denitrification, primarily due to acidification of the soils. Glob. Chang. Biol. 20, 1685–1698. https://doi.org/10.1111/gcb.12461.
Reay, D.S., Davidson, E.A., Smith, K.A., Smith, P., Melillo, J.M., Dentener, F., Crutzen, P. J., 2012. Global agriculture and nitrous oxide emissions. Nat. Clim. Chang. 2, 410–416. https://doi.org/10.1038/nclimate1458.
Ruser, R., Flessa, H., Russow, R., Schmidt, G., Buegger, F., Munch, J.C., 2006. Emission of N_2O, N_2 and CO_2 from soil fertilized with nitrate: Effect of compaction, soil moisture and rewetting. Soil Biol. Biochem. 38, 263–274. https://doi.org/10.1016/j.soilbio.2005.05.005.
Ruser, R., Fuß, R., Andres, M., Hegewald, H., Kesenheimer, K., Köbke, S., Räbiger, T., Quinones, T.S., Augustin, J., Christen, O., Dittert, K., Kage, H., Lewandowski, I., Prochnow, A., Stichnothe, H., Flessa, H., 2017. Nitrous oxide emissions from winter oilseed rape cultivation. Agric. Ecosyst. Environ. 249, 57–69.
Schlichting, E., Blume, H., Stahr, K., 1995. Soils Practical. Blackwell.
Senbayram, M., Chen, R., Budai, A., Bakken, L., Dittert, K., 2012. N_2O emission and the $N_2O/(N_2O+N_2)$ product ratio of denitrification as controlled by available carbon substrates and nitrate concentrations. Agric. Ecosyst. Environ. 147, 4–12. https://doi.org/10.1016/j.agee.2011.06.022.
Shcherbak, I., Millar, N., Robertson, G.P., 2014. Global metaanalysis of the nonlinear response of soil nitrous oxide (N_2O) emissions to fertilizer nitrogen. Proc. Natl. Acad. Sci. U. S. A. 111, 9199–9204. https://doi.org/10.1073/pnas.1322434111.
Šimek, M., Jíšová, L., Hopkins, D.W., 2002. What is the so-called optimum pH for denitrification in soil? Soil Biol. Biochem. 34, 1227–1234. https://doi.org/10.1016/S0038-0717(02)00059-7.
Skinner, C., Gattinger, A., Krauss, M., Krause, H.M., Mayer, J., van der Heijden, M.G.A., Mäder, P., 2019. The impact of long-term organic farming on soil-derived greenhouse gas emissions. Sci. Rep. 9, 1–10. https://doi.org/10.1038/s41598-018-38207-w.
Sommer, M., Gerke, H.H., Deumlich, D., 2008. Modelling soil landscape genesis — A "time split" approach for hummocky agricultural landscapes. Geoderma 145, 480–493. https://doi.org/10.1016/j.geoderma.2008.01.012.
Sommer, M., Augustin, J., Kleber, M., 2016. Feedbacks of soil erosion on SOC patterns and carbon dynamics in agricultural landscapes-The CarboZALF experiment. Soil Tillage Res. 156, 182–184. https://doi.org/10.1016/j.still.2015.09.015.
Song, H.e., Wang, J., Zhang, K., Zhang, M., Hui, R., Sui, T., Yang, L., Du, W., Dong, Z., 2020. A 4-year field measurement of N_2O emissions from a maize-wheat rotation system as influenced by partial organic substitution for synthetic fertilizer. J. Environ. Manage. 263 https://doi.org/10.1016/j.jenvman.2020.110384.
Song, Y., Zou, Y., Wang, G., Yu, X., 2017. Soil Biology & Biochemistry Altered soil carbon and nitrogen cycles due to the freeze-thaw effect: A meta-analysis. Soil Biol. Biochem. 109, 35–49. https://doi.org/10.1016/j.soilbio.2017.01.020.
Stehfest, E., Bouwman, L., 2006. N_2O and NO emission from agricultural fields and soils under natural vegetation: Summarizing available measurement data and modeling of global annual emissions. Nutr. Cycl. Agroecosystems 74, 207–228. https://doi.org/10.1007/s10705-006-9000-7.
Tian, H., Xu, R., Canadell, J.G., Thompson, R.L., Winiwarter, W., Suntharalingam, P., Davidson, E.A., Ciais, P., Jackson, R.B., Janssens-Maenhout, G., Prather, M.J., Regnier, P., Pan, N., Pan, S., Peters, G.P., Shi, H., Tubiello, F.N., Zaehle, S., Zhou, F., Arneth, A., Battaglia, G., Berthet, S., Bopp, L., Bouwman, A.F., Buitenhuis, E.T., Chang, J., Chipperfield, M.P., Dangal, S.R.S., Dlugokencky, E., Elkins, J.W., Eyre, B. D., Fu, B., Hall, B., Ito, A., Joos, F., Krummel, P.B., Landolfi, A., Laruelle, G.G., Lauerwald, R., Li, W., Lienert, S., Maavara, T., MacLeod, M., Millet, D.B., Olin, S., Patra, P.K., Prinn, R.G., Raymond, P.A., Ruiz, D.J., van der Werf, G.R., Vuichard, N., Wang, J., Weiss, R.F., Wells, K.C., Wilson, C., Yang, J., Yao, Y., 2020. A comprehensive quantification of global nitrous oxide sources and sinks. Nature 586 (7828), 248–256.
Ussiri, D., Lal, R., 2012. Soil emission of nitrous oxide and its mitigation. Soil Emission of Nitrous Oxide and its Mitigation. https://doi.org/10.1007/978-94-007-5364-8_1.
Vaidya, S., Schmidt, M., Rakowski, P., Bonk, N., Verch, G., Augustin, J., Sommer, M., Hoffmann, M., 2021. A novel robotic chamber system allowing to accurately and precisely determining spatio-temporal CO_2 flux dynamics of heterogeneous croplands. Agric. For. Meteorol. 296, 108206 https://doi.org/10.1016/j.agrformet.2020.108206.
Van Groenigen, J.W., Kasper, G.J., Velthof, G.L., Van Den Pol-Van Dasselaar, A., Kuikman, P.J., 2004. Nitrous oxide emissions from silage maize fields under different mineral nitrogen fertilizer and slurry applications. Plant Soil 263, 101–111. https://doi.org/10.1023/B:PLSO.0000047729.43185.46.
Van Oost, K., Quine, T.A., Govers, G., De Gryze, S., Six, J., Harden, J.W., Ritchie, J.C., McCarty, G.W., Heckrath, G., Kosmas, C., Giraldez, J.V., Marques Da Silva, J.R., Merckx, R., 2007. The impact of agricultural soil erosion on the global carbon cycle. Science (80-) 318, 626–629. https://doi.org/10.1126/science.1145724.
Vdlufa Methodenbuch I. Die Untersuchung von Böden (Handbook: Soil Analysis) 1991 Darmstadt (Germany).
Venterea, R.T., Petersen, S.O., Klein, C.A.M., Pedersen, A.R., Noble, A.D.L., Rees, R.M., Gamble, J.D., Parkin, T.B., 2020. Global Research Alliance N_2O chamber methodology guidelines: Flux calculations. J. Environ. Qual. 49 (5), 1141–1155.
Vilain, G., Garnier, J., Tallec, G., Cellier, P., 2010. Effect of slope position and land use on nitrous oxide (N_2O) emissions (Seine Basin, France). Agric. For. Meteorol. 150, 1192–1202. https://doi.org/10.1016/j.agrformet.2010.05.004.
Wang, X., Cammeraat, E.L.H., Kalbitz, K., 2020. Erosional effects on distribution and bioavailability of soil nitrogen fractions in Belgian Loess Belt. Geoderma 365, 114231. https://doi.org/10.1016/j.geoderma.2020.114231.
Weintraub, S.R., Taylor, P.G., Porder, S., Cleveland, C.C., Asner, G.P., Townsend, A.R., 2015. Topographic controls on soil nitrogen availability in a lowland tropical forest. Ecology 96, 1561–1574. https://doi.org/10.1890/14-0834.1.

Weller, S., Fischer, A., Willibald, G., Navé, B., Kiese, R., 2019. N_2O emissions from maize production in South-West Germany and evaluation of N_2O mitigation potential under single and combined inhibitor application. Agric. Ecosyst. Environ. 269, 215–223. https://doi.org/10.1016/j.agee.2018.10.004.

Wrb, 2015. World reference base for soil resources 2014, International soil classification system, No. 106. World Soil Resources Reports, Rome.

Xue, Z., Cheng, M., An, S., 2013. Soil nitrogen distributions for different land uses and landscape positions in a small watershed on Loess Plateau. China. Ecol. Eng. 60, 204–213. https://doi.org/10.1016/j.ecoleng.2013.07.045.

Zhou, M., Zhu, B., Wang, S., Zhu, X., Vereecken, H., Brüggemann, N., 2017. Stimulation of N_2O emission by manure application to agricultural soils may largely offset carbon benefits: a global meta-analysis. Glob. Chang. Biol. 23, 4068–4083. https://doi.org/10.1111/gcb.13648.